

Article

Spatial Distribution and the Key Impact Factors of Soil Selenium of Cultivated Land in Lianyuan City, China

Siyu Guo ¹, Xinyue Chen ^{1,*}, Zhijia Lin ^{2,*}, Feng Yin ¹, Pengyuan Jia ² and Keyun Liao ²

¹ School of Earth Sciences and Spatial Information Engineering, Hunan University of Science and Technology, Xiangtan 411201, China; 21010103010@mail.hnust.edu.cn (S.G.); yinfeng@hnust.cn (F.Y.)

² Geological Survey Institute of Hunan Province, Changsha 410014, China; jiapengyuan@hnsdzty5.wecom.work (P.J.); liaokeyun@hnsdzty5.wecom.work (K.L.)

* Correspondence: chenxinyue@hnust.edu.cn (X.C.); linzhijia@mails.ucas.edu.cn (Z.L.)

Abstract: Selenium (Se) is a micronutrient that has attracted significant attention, because the threshold for human health is low. During soil surveys in China, large areas of low-Se soil were found, and this condition may increase the probability of people suffering from Se deficiency. A multi-purpose regional geochemical survey conducted in the Lou Shao basin of Hunan Province found abundant Se-rich soils in Lianyuan City. However, as the primary grain-producing area in Hunan Province, the key factors affecting the spatial distribution of soil Se in the cultivated land of Lianyuan City remain to be elucidated. Therefore, based on the data of 5516 topsoil samples (0–20 cm) of cultivated land in Lianyuan City, we used geostatistics, correlation analysis, and a Geodetector to explore the effects of geological conditions (strata), soil types, soil properties, and topography on the distribution of Se in soil. The results showed that (1) in comparison to cultivated land in the Chinese mainland, Japan, Belgium, and Sweden, the cultivated land in Lianyuan City exhibits higher Se contents, with Se-sufficient and Se-rich areas accounting for 9.74% and 88.96% of the total area, respectively; (2) the distribution of high-Se soil was consistent with that in the Longtan Formation, Dalong Formation, and Daye Formation; (3) organic matter (OM) showed a positive correlation with Se, while both the elevation and slope were negatively correlated with Se; (4) stratum had the most significant effect on the spatial variation in soil Se, followed by OM. Lianyuan City is a typical Se-rich area, and the high level of Se in soil reduces the risk of local residents suffering with diseases caused by Se deficiency. The synergistic effect of stratum and OM is the key factor influencing Se enrichment in soils. Moreover, low-lying flat areas are more conducive to the accumulation of Se. This study will help farmers to identify suitable Se-rich cultivation areas in order to increase the Se content in crops, thereby providing a valuable basis for improvements in human health and the optimization of agricultural strategies.

Keywords: selenium; stratum; soil organic matter; Geodetector; Lianyuan



Citation: Guo, S.; Chen, X.; Lin, Z.; Yin, F.; Jia, P.; Liao, K. Spatial Distribution and the Key Impact Factors of Soil Selenium of Cultivated Land in Lianyuan City, China. *Agriculture* **2024**, *14*, 686. <https://doi.org/10.3390/agriculture14050686>

Academic Editor: Dane Lamb

Received: 14 March 2024

Revised: 22 April 2024

Accepted: 24 April 2024

Published: 27 April 2024



Copyright: © 2024 by the authors. Licensee MDPI, Basel, Switzerland. This article is an open access article distributed under the terms and conditions of the Creative Commons Attribution (CC BY) license (<https://creativecommons.org/licenses/by/4.0/>).

1. Introduction

Se has multiple biological functions (antioxidant, immunoregulation, antagonism, etc.) and is a crucial micronutrient for the normal operation of human physiological functions [1,2]. Because of its significant efficacy, Se has been studied in geology, ecology, chemistry, agriculture, and medicine for over 190 years [3,4]. The levels of Se that are safe for human consumption fall within a narrow range, as both excessive and insufficient intake can lead to illness. To reduce the risk of hypertension, hyperglycemia, cancer, and Keshan disease, the World Health Organization (WHO) recommends a minimum daily selenium intake of 19 µg for adults, taking weight into account, with specific doses of 21 µg for men and 16 µg for women [5]. Additionally, 400 µg has been established as the upper limit of daily Se intake for adults, and exceeding this threshold (400 µg) can lead to hair loss, severe liver damage, defluvium unguium, and brain edema [6,7].

In soil, Se exists in either the inorganic form (ionic) or the organic form. Once absorbed in plants, it enters the human body through the food chain [8,9]. Therefore, human Se intake is primarily dictated by the Se content in soil [10]. However, the distribution of Se in soil is extremely uneven. Due to varied geological and geographical characteristics, the Se content in soil fluctuates significantly across regions. In regions with naturally low levels of Se in the soil, biofortification programs are often implemented for the purpose of enhancing dietary Se intake. The latest research has estimated that 51% of China's land mass lacks Se [11,12]. Compared to statistics from 1989, which indicated that 72% of China's soil was deficient in Se, there has been a significant improvement in the rates of Se deficiency in soil. However, more than half of the soil in China still lacks Se. Meanwhile, over 0.15 billion people are facing the harmful consequences of Se deficiency [13]. Thus, it is of great importance to understand the key factors affecting Se distribution to increase human Se intake and protect human health.

The factors affecting soil Se distribution are not singular. Among them, parent material is usually considered the most important influence on Se levels in soil [10,14]. Se-rich soil can be formed through the weathering of Se-rich rocks [15]. For example, the enrichment of Se in the Enshi area is related to black carbon-siliceous rock formed during the Permian period [16]. The distribution of Se in the soil of Taoyuan, Hunan Province, is controlled by Lower Cambrian and Ediacaran black rock [17]. Moreover, Xia et al. also found that soils developed from the black rock series of Sinian and Lower Cambrian have a higher Se content than soils developed from other parent rocks in Ningguo, Anhui Province [18].

The distribution of Se in soil is not exclusively determined by its parent material. Se in soil is also influenced by environmental factors such as soil properties, soil type, topography, and precipitation [19,20]. The pH and soil OM content substantially influence the characteristics and functionalities of soil, acting as crucial physicochemical indicators in soil analyses. Several studies [21–23] have shown that the chemical speciation of Se can easily be transformed into selenite (Se^{4+}) with weak migration ability when the soil pH rises, resulting in the increase in Se contents in soil. Adsorption and immobilization are important approaches for OM to control Se. In OM-rich soil, Se binds with humic substances through adsorption, cation bridging, and coordination, thereby forming stable complexes that reduce Se leaching. Furthermore, Wang et al. revealed that the high OM content is the main reason for Se enrichment in dark-brown earth and black soils [24].

The soil type determines the properties of the soil, which determine the change in Se content. The Se content is low in the less developed and sandiest soil, such as Pozzols, Arenosols, and Regosols. Topography is a comprehensive embodiment of the regional environment and indirectly influences the distribution of soil Se through the redistribution of minerals, water, and energy in local areas [25–27]. For instance, river terraces formed in the Quaternary period, in which intense leaching occurred during soil formation, have low levels of Se in the soil [28]. In contrast, in situ weathered soils in karst mountain and hilly areas have inherited the geochemical characteristics of Se-rich rocks. It has also been reported that precipitation contributes 5610 tons of Se to the land each year [29], thereby representing an important source of Se in soil. Additionally, precipitation also impacts soil moisture, clay content, and pH, which in turn affect the ability of the soil to store Se [19].

At present, numerous studies have been conducted to investigate the factors that affect soil Se distribution [30–32]. However, studies that quantify the effects of natural factors on soil Se distribution are inadequate. The cultivated land in Lianyuan City is predominantly used for the cultivation of cereals, including maize and rice. Consequently, Lianyuan City is recognized as one of the major grain-producing areas in Hunan Province. According to the multi-purpose regional geochemical survey conducted in the Lou Shao basin of Hunan Province, the average Se content in the topsoil of cultivated land in Lianyuan City was 0.727 mg/kg (unpublished data), showing great potential for the development of Se-rich agriculture. However, as a key city for Se-rich industry development, research into the spatial distribution and the key factors influencing Se has not been carried out in Lianyuan City's cultivated land. In this study, the Spearman correlation coefficient and

the Geodetector were used to assess the effects of stratum, soil type, soil properties, and topography on Se in the soil. Our research aims included (1) investigating the spatial distribution of Se in topsoil; (2) analyzing the relationship between Se and various natural factors (stratum, soil type, pH, OM, elevation (H), slope (SL), and topographic wetness index (TWI)); and (3) determining the key factors affecting the Se in the soil.

2. Materials and Methods

2.1. Study Area

Lianyuan City is situated in central Hunan Province (27°27′–28°20′ N, 111°33′–112°20′ E) (Figure 1a,b). It has a total area of 1830 km² and a subtropical monsoon climate, with an average annual temperature and average annual precipitation of 16–17.3 °C and 1420.3 mm, respectively. The mean annual duration of sunshine is 1557.4 h, with a sunshine rate of 35%. The terrain of this region is mostly mountainous and hilly (37.78% and 26.95% of the total area, respectively). The south, north, and west are mountainous, the central area is occupied by low mountains and hills, and the east is flat. The whole area resembles an “E” shape.

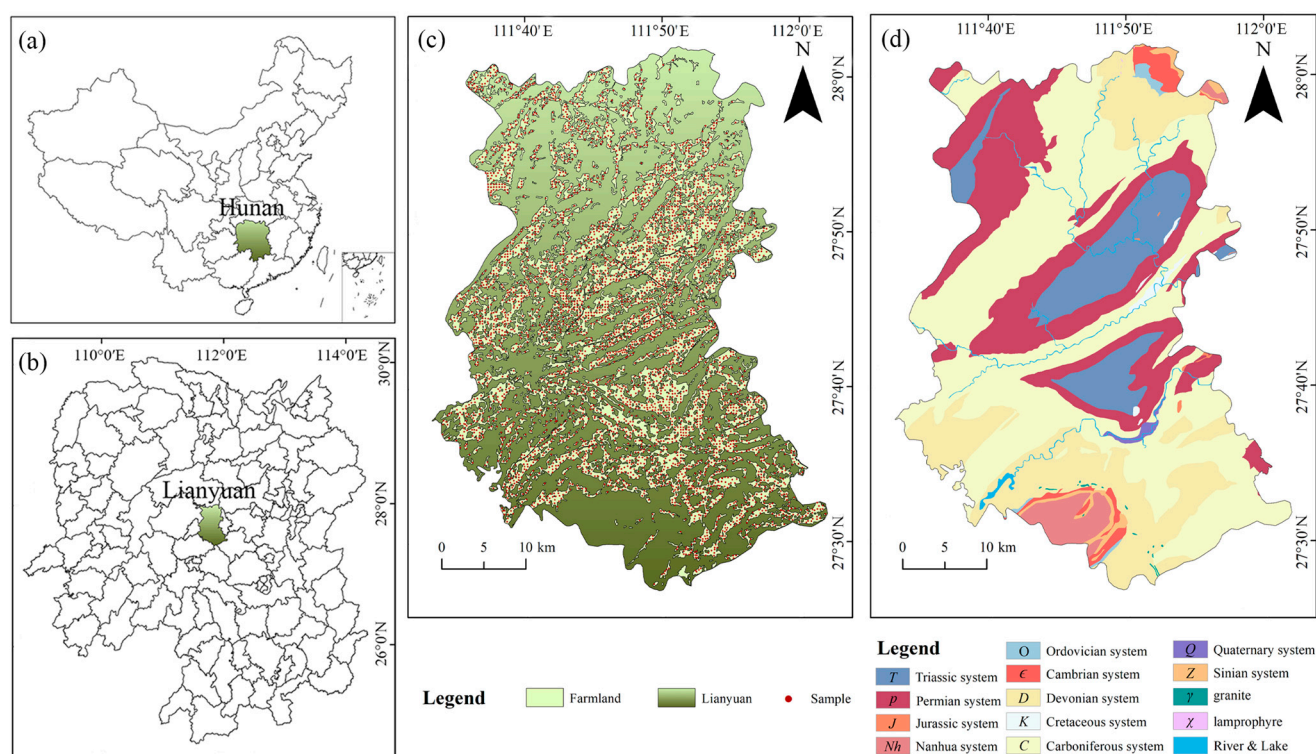


Figure 1. (a) Location of Hunan Province in China; (b) location of Lianyuan City in Hunan Province; (c) soil sampling sites of Lianyuan City; (d) simplified geological map.

Abundant rainfall in Lianyuan City readily induces desilicification and allitization in the soil. Red soil is the most dominant soil type, accounting for about 67.17% of the total soil area, most of which is concentrated in the mountains. Paddy soil, red calcareous soil, gray calcareous soil, and yellow soil make up the rest of the area.

Geologically, the study area was exposed from Proterozoic to Quaternary. The stratigraphic development of the Upper Paleozoic is complete (Figure 1d). Most of the land surface exposes at Carboniferous, followed by Devonian and Permian (Figure 1d). The lithology of the Carboniferous strata is limestone and dolomite, both of which are widely distributed throughout the study area. Carboniferous areas make up the axis of the anticlines. The Devonian consists of sandstone, shale, and limestone and is distributed throughout the southern part of the study area. The lithology in the Permian is mainly black rock series such as stone coal, which is thought to have high levels of Se.

2.2. Soil Sampling and Chemical Analyses

The soil data used in this study were taken from a multi-purpose regional geochemical survey conducted in the Lou Shao basin of Hunan Province. In this survey, topsoil samples (0–20 cm) were collected using a 1×1 km regular grid after considering soil type, topography, and other factors. In order to minimize errors, 3–5 topsoil samples were incorporated into a single sample for chemical analysis. A total of 5516 chemical analysis samples were obtained (Figure 1c). The average sampling density was 3 topsoil samples/km². All samples were air-dried in a laboratory. After plant roots and stones were separated from the soil, samples were sieved through a 200 mesh (<0.074 mm) for analysis. According to the specifications of the multi-purpose regional geochemical survey (DD2005-01), the chemical analysis of soil samples was carried out by the Geological Survey Institute of Hunan Province. The Se content in soil was determined via hydride generation atomic fluorescence spectrometry (HG-AFS). Soil pH was measured using a pH meter. Soil OM was determined using the potassium bichromate method.

In the process of sample determination, standard materials (GBW07376 (GSD-25), GBW07377 (GSD-26), GBW07378 (GSD-27), GBW07380 (GSD-29), GBW07381 (GSD-30), GBW07382 (GSD-31), GBW07383 (GSD-32), and GBW07384 (GSD-33)) were used to control the quality of the experiment, and blank samples were utilized in order to eliminate the influence of reagents. The absolute value of the relative standard deviation of the sample detection was less than 12.5%. The average recovery of Se was 92%. The accuracy and precision of all analytes met the requirements for quality outlined in the specification (DD2005-01).

2.3. Data Sources and Processing

The geological map of Lianyuan City is a modified version of the 1:200,000 geologic map (Linli map) downloaded from the National Geological Archives of China (<http://www.ngac.org.cn/> accessed on 20 October 2023). Data on soil type were obtained from the Soil Science Database (<http://vdb3.soil.csdb.cn/> accessed on 20 October 2023). The Digital Elevation Mode (DEM) data came from the China Geospatial Data Cloud and had a resolution of 30 m. The terrain factors (H, SL, TWI) were calculated, extracted, and arranged using ArcGIS10.7 (Figure 2). The slope was converted using the Spatial Analyst Tool in ArcGIS 10.7 (Figure 2b). SL values were divided into flat (<3°), flat gentle (3–8°), gentle (8–15°), gentle steep (15–25°), steep (25–35°), and sharp steep (>35°) [33]. TWI, as originally proposed by Beven and Kirk, was used to characterize soil moisture conditions (Figure 2c) [34]. Formula (1) was used as follows:

$$TWI = \ln \frac{SCA}{\tan \beta} \quad (1)$$

where SCA is the contributing area per unit length of the contour (m²/m); and β is the SL, in degrees, at a given point.

For each sampling site, information regarding geology and soil type was extracted using the extraction toolset in ArcGIS 10.7. Nevertheless, sampling sites were not entirely covered with the data sets of geology and soil type. As a result, the number of data points that can be used for the Se content statistics in various strata and soil types was less than the number of total sampling points. The amount of missing data (stratum: 50; soil types: 504) was far less than the total sampling points (5516 samples from the topsoil), so it was considered that the issue would not significantly impact the research results.

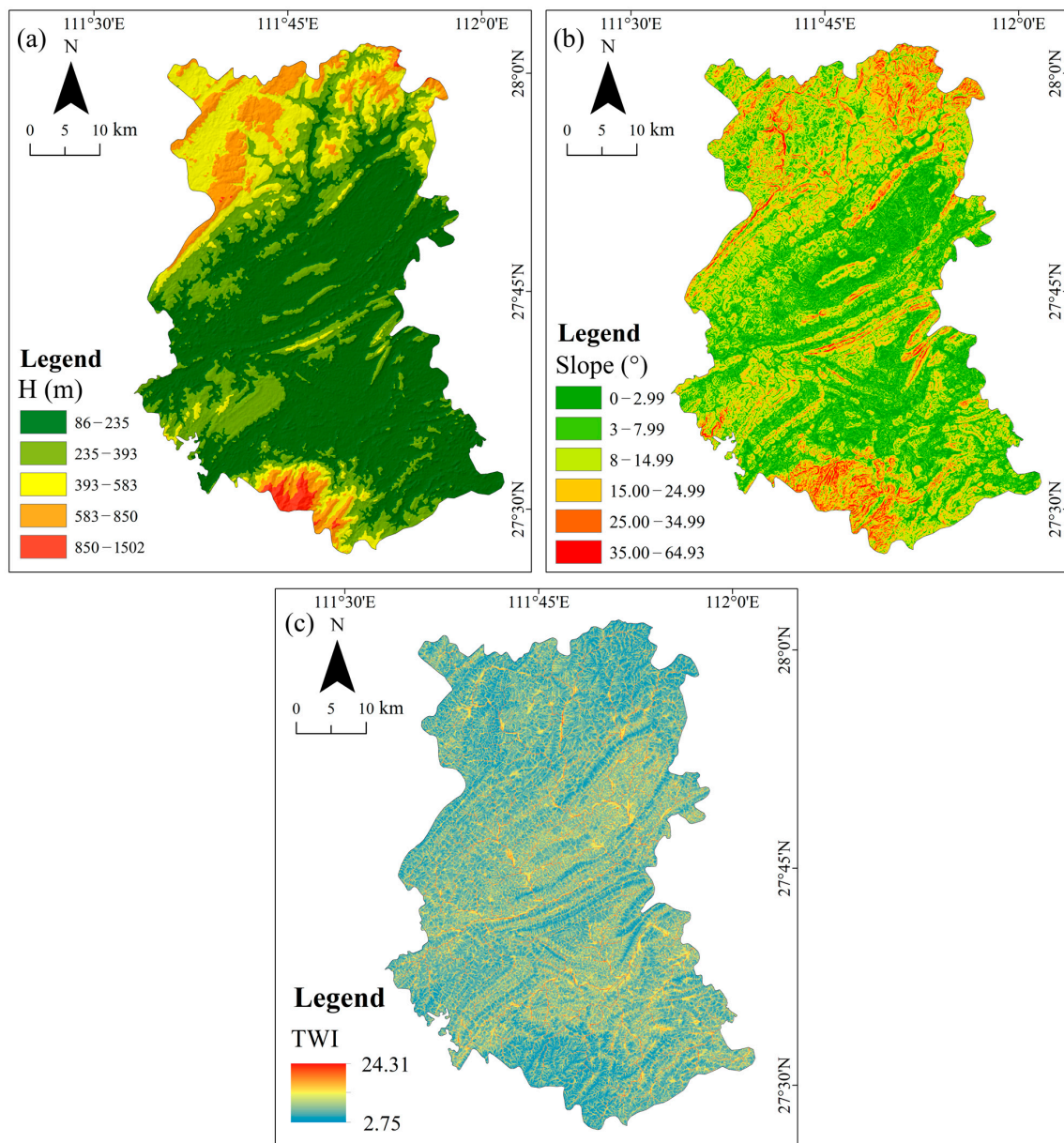


Figure 2. Topography in Lianyuan City. (a) H; (b) SL; (c) TWI. Note: H: elevation; SL: slope; TWI: topographic wetness index.

2.4. Geodetector

Geodetector is a new statistical method that has been extensively applied in studying the factors influencing the phenomena of nature, economy, and society [35]. The basic theory of Geodetector is to judge the similarity in the spatial distribution of two variables from the perspective of spatial stratified heterogeneity. More specifically, if an independent variable has an important influence on a dependent variable, then there should be a similarity in the spatial distribution of independent variables and dependent variables. The method is subject to fewer underlying assumptions, and has clear advantages when dealing with mixed-type data. Geodetector includes factor detector, interaction detector, ecological detector, and risk detector. In this paper, the factor detector and interaction detector were used to analyze the factors (stratum, soil type, pH, OM, H, SL, and TWI) influencing the distribution of Se content and their interactions.

The degree to which the independent variable (X) influenced the dependent variable (Y) was determined using a factor detector. The expression is given below in (2) and (3):

$$q = 1 - \frac{\sum_{h=1}^L N_h \delta_h^2}{N \delta^2} = 1 - \frac{SSW}{SST} \quad (2)$$

$$SSW = \sum_{h=1}^L N_h \delta_h^2; SST = N \delta^2 \quad (3)$$

where h ($h = 1, 2, \dots, L$) is the strata of independent variable (X) or dependent variable (Y); N_h and N are the number of units in an h strata and study area, respectively; δ_h^2 and δ^2 are the variances in Y in an h strata and study area, respectively. The value of q is strictly within $[0, 1]$, and $q = 0$ indicates that there is no coupling between Y and X, while $q = 1$ indicates that Y is completely determined by X.

The interaction detector reveals whether the risk factors X1 and X2 (and more X) have an interactive influence on a response variable Y. Value close to $q = 1$ indicates that Y is entirely determined by the risk factors of X1 and X2, and the value of $q = 0$ indicates that there is no coupling between Y and more X (X1 and X2). In this study, soil Se content is the dependent variable, and the independent variables (X) include stratum, soil type, soil pH, soil OM, H, SL, and TWI.

2.5. Statistical Analysis

IBM SPSS Statistics 27 and Excel 2016 were used to count and analyze the initial data. The Kolmogorov–Smirnov method was used to evaluate the normality of the Se content. The Spearman method was used to determine the correlation between Se content and various influencing factors.

Geodetector was downloaded from <http://www.geodetector.cn/> (accessed on 20 October 2023) to identify factors that significantly affect soil Se. Discretization tests were performed on each independent variable based on discrete methods (equal interval method, natural breaks method, standard deviation method, geometric interval method, and quantile method) in ArcGIS and classification methods in the relevant standards. The optimal scale of spatial data discretization was selected. The classification method with the largest q value was chosen as the optimal parameter for the analysis of influencing factors. Soil Se content (the dependent variable) is on the second line, followed by influencing factors (independent variables), including stratum, soil type, soil properties (pH, OM), and topographic parameters (H, SL, TWI). The classification methods and results of the influencing factors are presented in Table 1.

Table 1. The classification results of impact factors.

Factors	Se (mg/kg)	S	ST	pH	OM (g/kg)	H (m)	SL (°)	TWI
1	0.058–0.520	K	CM	<5	<6	98–157	<3	3.70–5.70
2	0.521–0.738	Є	FR	5–6.5	6–10	158–198	3–8	5.71–6.19
3	0.739–1.081	O	AT	6.5–7.5	10–20	199–252	8–15	6.20–6.63
4	1.082–1.716	D	—	7.5–8.5	20–30	253–325	15–25	6.64–7.07
5	1.717–2.830	Q	—	≥8.5	—	326–416	25–35	7.08–7.62
6	2.831–4.412	T	—	—	—	417–506	>35	7.63–8.50
7	4.413–6.760	P	—	—	—	507–610	—	8.51–9.89
8	6.761–12.040	C	—	—	—	611–835	—	9.90–20.29
Classification methods	Equal interval	[36]	[37]	[38]	[39]	Equal interval	[33]	Quantile

Note: S: stratum; K: Cretaceous; Є: Cambrian; O: Ordovician; D: Devonian; Q: Quaternary; T: Triassic; P: Permian; C: Carboniferous; ST: soil type; CM: Cambisols; FR: Ferralsols; AT: Anthrosols; OM: organic matter; H: elevation; SL: slope; TWI: topographic wetness index.

3. Results and Discussion

3.1. Se contents in Topsoil

After the Kolmogorov–Smirnov normality test, the Se content in the topsoil was non-normally distributed ($p < 0.05$) (Figure 3a). Subsequently, the logarithmic transformation of Se content in topsoil was performed. Although the Se logarithm demonstrated a trend toward normal distribution, it also did not pass the Kolmogorov–Smirnov normality test ($p < 0.05$) (Figure 3b). The Se content in topsoil ranged from 0.06 to 12.04 mg/kg, with a mean value of 0.73 mg/kg and a median value of 0.61 mg/kg. Due to the skewness of the distribution data, the median, rather than the average, was selected to evaluate the overall level of Se in the study area. The coefficient of variation (CV) for Se was 83%. According to the classification of variation degree [40], Se content was highly variable, indicating that the Se content in topsoil is unstable. The uneven geological distribution of Se-bearing minerals may contribute to the high variability of Se in soil. This finding is consistent with that of Williams et al. [19].

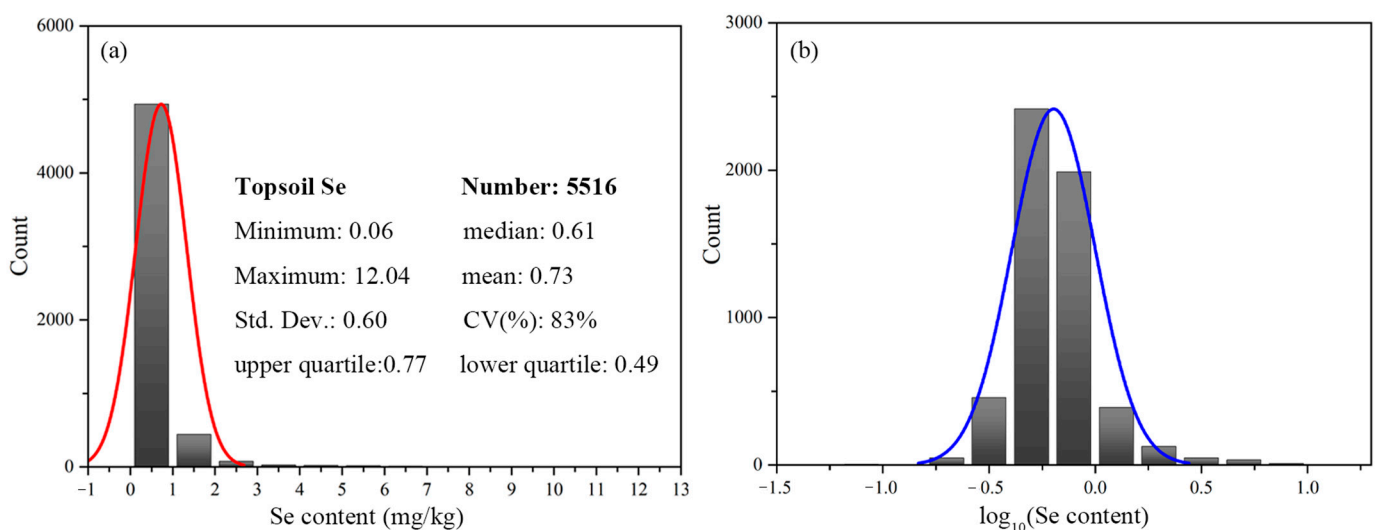


Figure 3. (a) Descriptive statistics and frequency distribution of Se content in cultivated land's topsoil; (b) frequency distribution of Se content after logarithmic transformation. Note: the red and blue lines represent normal distribution curves.

The Se content in soil is crucial for the accumulation of Se in plants. The existing research shows that plants absorb Se through the roots and accumulate it mainly in edible parts, such as the stems and leaves, rather than the roots [9]. This accumulation pattern closely links the Se content in plants' edible parts with the Se content in the soil. Therefore, precise management of soil Se levels is essential for ensuring an effective supply of Se to humans through the food chain.

Se plays a unique biological role and is indispensable for human health. Optimal intake of Se is of significant importance in maintaining human health, enhancing immune function, and preventing chronic diseases. However, ingesting Se in volumes outside the safe range may threaten human health. Se deficiency causes a series of endemic diseases (e.g., Keshan disease and Kashin–Beck disease). Likewise, excessive Se can trigger chronic selenosis.

In order to predict possible health risks in the study area, the Se content of cultivated land topsoil from Lianyuan City was compared with that in some representative areas. The topsoil Se content in the study area (0.61 mg/kg) was higher than the background soil level in China (0.290 mg/kg) (Table 2). Regional differences in soil Se levels are observed in cultivated lands worldwide. The Se content of cultivated land's topsoil in Lianyuan City was 2.54, 1.20, 0.97, 1.85, and 2.03 times that of mainland China, Japan, Scotland, Belgium, and Sweden, respectively. The Se in the topsoil of cultivated land in Lianyuan City was higher than that in Jiangjin, Chongqing Province (longevity area), and lower than that in Yongfu, Guangzhou Province (longevity area) (Table 2). Rangtang, Sichuan Province, and

Changdu, Xizang Autonomous Region are areas that suffer with Kaschin–Beck disease. The topsoil Se of the cultivated land in Lianyuan City was 4.07 and 2.44 times that in Rangtang and Changdu (Table 2), suggesting that residents of Lianyuan City are less at risk of suffering with Kaschin–Beck disease. Furthermore, the level of topsoil Se in cultivated land in Lianyuan City was considerably lower than that in areas that see frequent cases of selenosis (Ziyang, Shanxi Province and Yutangba, Hubei Province) and was 1.85 times and 0.60 times higher than in cultivated land in Longshan and Shimen, which are typical Se-rich areas in Hunan Province (Table 2). In summary, the Se content in the study area is relatively high. Regarding the risk of selenosis, further studies need to be carried out in combination with soil Se speciation and crop Se content.

Table 2. Se content in cultivated land topsoil from Lianyuan City and other area of China and world (mg/kg).

Region	Se	Source	Health
Lianyuan (cultivated land)	0.06~12.04 (0.61)	This study	–
Japan (cultivated land)	0.05~2.80 (0.51)	[41]	–
Scotland (cultivated land)	0.19~1.46 (0.63)	[42]	–
Belgium (cultivated land)	0.14~0.70 (0.33)	[43]	–
Sweden (cultivated land)	<0.05~13.30 (0.30)	[44]	–
Chinese mainland (cultivated land)	0.01~16.24 (0.24)	[45]	–
Longshan, Hunan (cultivated land)	0.18~0.69 (0.33)	[46]	–
Shimen, Hunan (cultivated land)	0.04~8.55 (1.02)	[47]	–
Changdu, Xizang	0.11~0.46 (0.25)	[48]	Kashin–Beck disease
Rangtang, Sichuan	0.09~0.26 (0.15)	[49]	Kashin–Beck disease
Ziyang, Shanxi	0.50~16.96 (4.78)	[50]	Selenosis
Yutangba, Hubei	0.41~42.3 (4.75)	[51]	Selenosis
Jiangjin, Chongqing	0.04~1.11 (0.32)	[52]	Longevity area
Yongfu, Guangzhou	0.27~1.40 (0.80)	[53]	Longevity area

3.2. Spatial Distribution of Se in Topsoil

Using soil sample data from cultivated land in Lianyuan City, the overall geographic distribution pattern of topsoil Se was mapped (Figure 4a). The topsoil Se content of cultivated land in various townships is summarized in Table 3. Higher Se contents were distributed within a ring occupying eight townships in the central part of the study area, including Shimashan, Qixingjie, and Longtang, among others (Figure 4a and Table 3). Lower Se contents were sporadically distributed in the north and south of the study area, occupying Fukou and Jinshi, among others (Figure 4a and Table 3). Overall, across cultivated land in Lianyuan City, Se contents were high in the central area and low in the north and south.

According to the classification standard of soil Se abundance and deficiency, the topsoil Se of cultivated land in Lianyuan City is categorized as Se-deficient (<0.125 mg/kg), Se-marginal (0.125–0.175 mg/kg), Se-sufficient (0.175–0.4 mg/kg), Se-rich (0.4–3.0 mg/kg), or Se-excessive (>3.0 mg/kg) (Figure 4b). The Se-deficient areas and the Se-marginal areas are very few, accounting for 0.07% and 0.02% of the cultivated land in Lianyuan City, and these values are insignificant and can largely be ignored. The Se-sufficient area occupies 9.74% of the cultivated land in Lianyuan City, primarily concentrated in the northern part of Lianyuan City. The Se-rich area is the largest and accounts for 88.96% of the cultivated land in Lianyuan City. The Se-excessive area is a small area gathered in the south and west, accounting for 1.21% of the cultivated land in Lianyuan City. Overall, the study area has a high Se level. Nearly 99% of the cultivated land is Se-rich and Se-sufficient. Spatial disparities in Se levels are likely influenced by factors such as varying parent materials, topography, and climate, all of which impact the sources and retention of Se [54]. Indeed, China faces widespread Se deficiency. The median Se content (0.171 mg/kg) [11] in Chinese soils is below the mean value in soil globally (0.400 mg/kg) [55]. In a study of the distribution pattern of soil Se concentration in China [12], it was found that the soil in

Lianyuan City is primarily Se-rich and Se-sufficient, which again supports the findings of this paper. In conclusion, under the premise of reasonable development, the cultivated land of Lianyuan City shows great potential for the cultivation of naturally Se-rich agricultural products. In addition, in order to avoid residents being poisoned through consumption of crops with excessive Se, the crops planted on the soil in the Se-excessive area should be tested for safety.

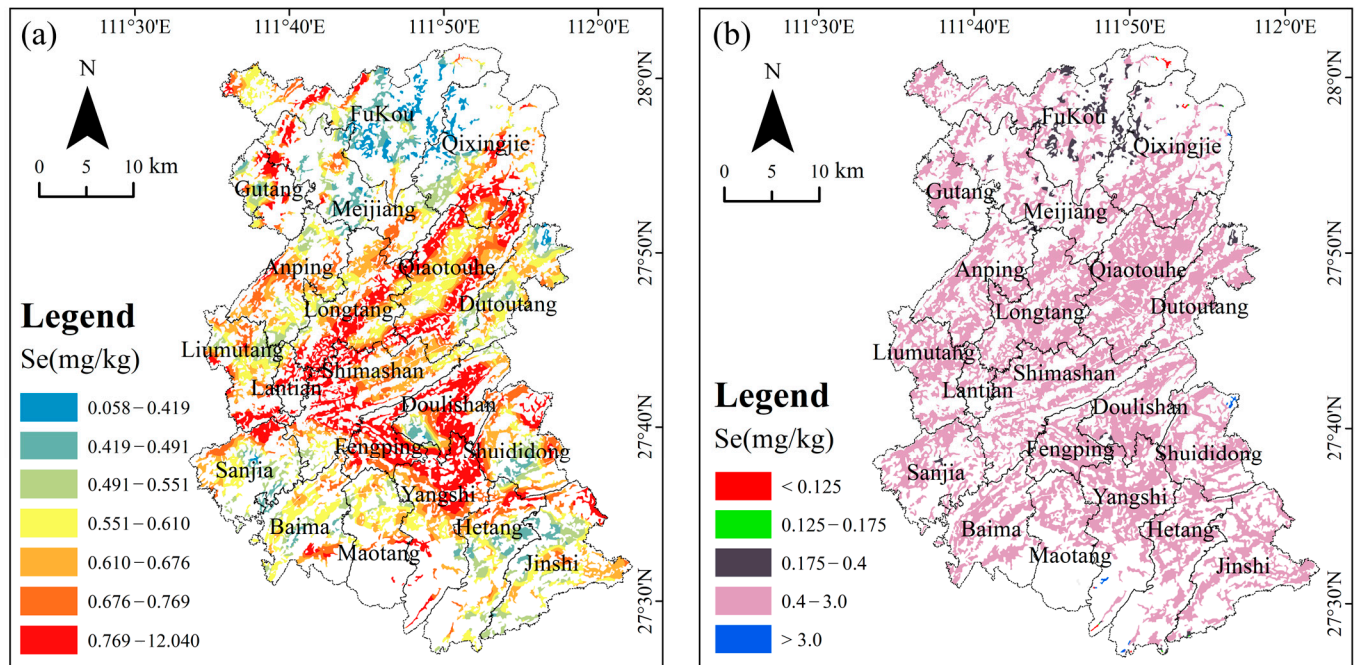


Figure 4. (a) Geochemical map of topsoil Se in cultivated land; (b) classification map of topsoil Se contents of cultivated land.

Table 3. Summary of topsoil Se contents of cultivated land on the township level in Lianyuan City (mg/kg).

Township	Min	Max	Mean
Anping	0.19	2.50	0.63
Baima	0.21	3.48	0.61
Doulishan	0.26	5.9	0.89
Dutoutang	0.10	1.5	0.58
Fengping	0.21	5.25	1.09
Fukou	0.15	6.36	0.58
Gutang	0.25	9.33	0.87
Hetang	0.24	6.68	0.63
Jinshi	0.07	5.47	0.66
Lantian	0.32	6.76	1.34
Liumutang	0.24	2.04	0.66
Longtang	0.08	8.63	0.90
Maotang	0.22	1.44	0.61
Meijiang	0.20	6.41	0.66
Qiaotouhe	0.24	5.69	0.82
Qixingjie	0.19	2.46	0.67
Sanjia	0.06	1.71	0.60
Shimashan	0.27	12.04	0.87
Shuididong	0.18	2.04	0.64
Yangshi	0.29	5.56	0.84

3.3. Influencing Factors of Se Content in Topsoil

3.3.1. Relationship of Regional Geology with Se Contents in Topsoil

The parent rock is the material basis for the formation of soil, so it is considered a key factor affecting soil Se. Due to the varied parent rocks in different geological units, Se appears in different contents in each geological unit. Here, the differences in soil Se content between geological units were compared (Figure 5). Permian topsoil had the highest Se content, with a mean and median of 1.01 mg/kg and 0.72 mg/kg, respectively (Table 4), indicating that the topsoil Se is highly dispersible. The Se content in Permian parent rocks may vary greatly, causing significant differences between the mean and median. The Se content in Ordovician topsoil was the lowest, with an average and median of 0.39 mg/kg and 0.36 mg/kg, respectively. Areas with high Se content coincided with the location of several strata (i.e., Permian Longtan Formation, Permian Dalong Formation, and Triassic Daye formation). The positional relationship is shown in Figure 6A,B.

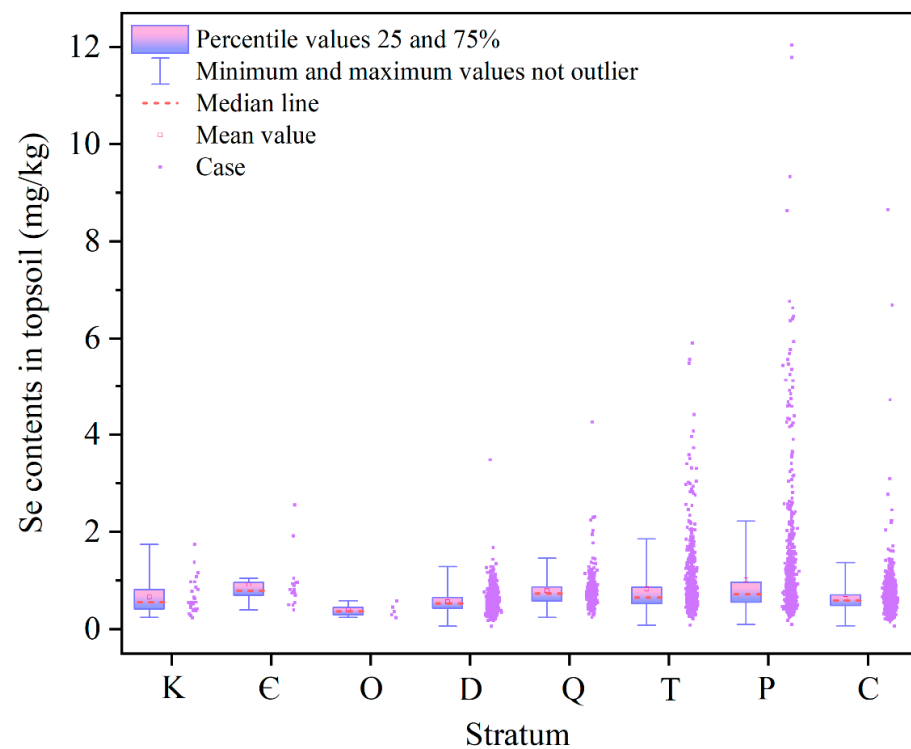


Figure 5. Boxplot of Se contents in topsoil according to geological units. Note: K: Cretaceous; E: Cambrian; O: Ordovician; D: Devonian; Q: Quaternary; T: Triassic; P: Permian; C: Carboniferous.

Table 4. The statistical parameters of topsoil Se contents in various geological units.

S	Number	Mean	Median	SD	Min	Max	Skewness	Kurtosis
K	29	0.65	0.55	0.35	0.24	1.74	1.50	2.31
E	18	0.92	0.79	0.52	0.39	2.55	2.31	5.71
O	5	0.39	0.36	0.14	0.24	0.58	0.62	−0.45
D	1059	0.56	0.53	0.21	0.06	3.48	3.41	38.32
Q	276	0.79	0.73	0.37	0.24	4.26	4.06	29.28
T	850	0.83	0.65	0.60	0.08	5.90	3.82	20.21
P	1068	1.01	0.72	1.06	0.10	12.04	4.86	32.36
C	2161	0.63	0.59	0.32	0.07	8.65	12.40	261.79

Note: S: stratum; K: Cretaceous; E: Cambrian; O: Ordovician; D: Devonian; Q: Quaternary; T: Triassic; P: Permian; C: Carboniferous.

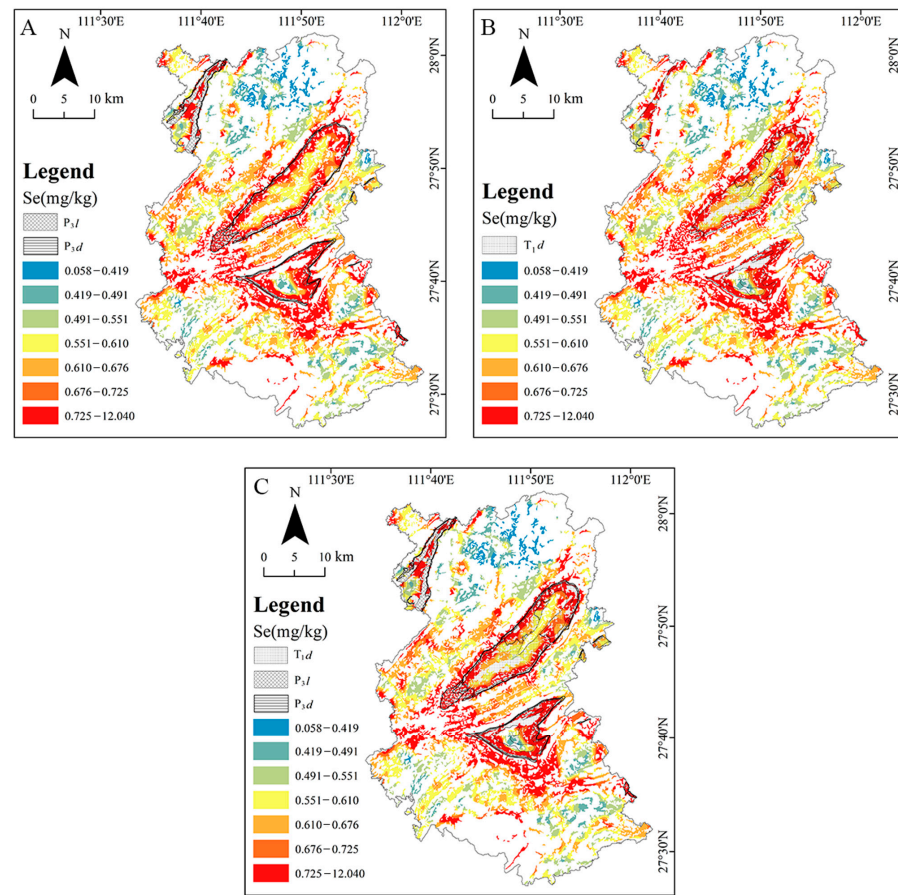


Figure 6. Geochemical map of Se in topsoil with stratigraphic boundary. (A) P_{3l} and P_{3d} ; (B) T_{1d} ; (C) P_{3l} , P_{3d} , and T_{1d} . Note: P_{3l} : Longtan Formation; P_{3d} : Dalong Formation; T_{1d} : Daye Formation.

Permian is an essential coal-forming period characterized by intense structural movement and frequent large-scale biological extinction events [56–58]. The Permian Longtan Formation is mainly composed of stone coal, carbonaceous shale, black siliceous shale, black siltstone, and sandy shale. The major lithologies of the Permian Dalong Formation are black siliceous shale, calcareous shale, and siliceous limestone. Black rock series are regarded as the primary geological sources of Se enrichment on Earth, and they are rich in OM [59–63]. The background values for Se in black rock series have not been published; however, Wang et al. reported that the mean content of Se in Chinese coal is as high as 3.91 mg/kg [64]. Cui et al. noted that the average Se content of black shale was 16 mg/kg in Ziyang, Shaanxi Province [65]. Ni et al. found that the average Se content of black shales and black siliceous rocks in Taoyuan, Hunan Province were 21.59 mg/kg and 2.91 mg/kg, respectively [17]. These values are well above the Se content of the upper continental crust [66], indicating that black rock series have a high Se content. Additionally, Zhu et al. discovered that an Se-excessive area was located in the Permian containing carbonaceous shale and stone coal in Yutangba, Hubei Province [51]. Thus, the high-Se soil from the substrate of the Longtan Formation and Dalong Formation is likely to be the product of Se-rich black rock series.

Limestone, dolomite, and shale are the main lithologies of the Triassic strata. Among them, limestone and dolomite belong to typical carbonate rocks. Xia et al. found that the Se content of carbonate rocks was low [67]. Se contents were found in the following rock types in descending order: slate > clay rocks > basic and ultra-basic rocks > alkaline rocks > basalt > granite > hypersthene sandstone > carbonate rock [24]. However, soil with a high Se content may also develop from carbonate rocks such as those in the southwestern parts of Guangxi Province [68] and the southern part of Guizhou Province [69]. Owing to the

unique chemical composition, carbonate rocks are susceptible to significant weathering during the formation of soil. Soil developed in areas of carbonate rock has a high degree of maturation, significant allitization, and a sticky texture, which means Se released during the weathering of parent rock is more easily retained. Jia et al. concluded that the formation of Se-rich soil in Anhui Province is related to the combination of the Se-rich rock stratum and the carbonate rock stratum [70]. Se-rich rocks provide Se for the soil, and the soil developed from carbonate rock plays the role of adsorption and fixation. In the present study, the Longtan Formation (black rock series), Dalong Formation (black rock series), and Daye Formation (carbonate rock) were observed to be adjacent (Figure 6C). Consequently, the high-Se soil from the Daye Formation substrate is most probably a consequence of the combined action of the Longtan Formation black rock series, Dalong Formation black rock series, and Daye Formation carbonate rock.

3.3.2. Relationship of Soil Type with Se Contents in Topsoil

The statistical parameters of Se contents in the WRB reference soil group are shown in Table 5. A corresponding box line diagram is presented in Figure 7. The mean Se content of different soil types decreased in the following order: Anthrosols > Ferralsols > Cambisols. The soil properties of Anthrosols, Ferralsols and Cambisols differ from one another. Cambisols have a low degree of development, high alkalinity, low clay mineral content, and high sand content. In contrast, Ferralsols are characterized by high development, low alkalinity, and abundant Fe-Al oxides and OM. The OM content of Anthrosols is high because of the double action of bioaccumulation and organic fertilizer. Thus, the mean Se content of Anthrosols and Ferralsols was higher than that of Cambisols, a result consistent with the findings of Gong et al. [54].

Table 5. Statistical parameters of topsoil Se content in various soil types.

Soil Type	Number	Max	Min	Mean	Median	SD	Skewness	Kurtosis
CM	407	3.90	0.18	0.60	0.53	0.33	4.70	34.45
FR	944	12.04	0.10	0.72	0.59	0.74	7.81	84.72
AT	3663	11.79	0.06	0.75	0.63	0.60	7.19	78.91

Note: CM: Cambisols; FR: Ferralsols; AT: Anthrosols.

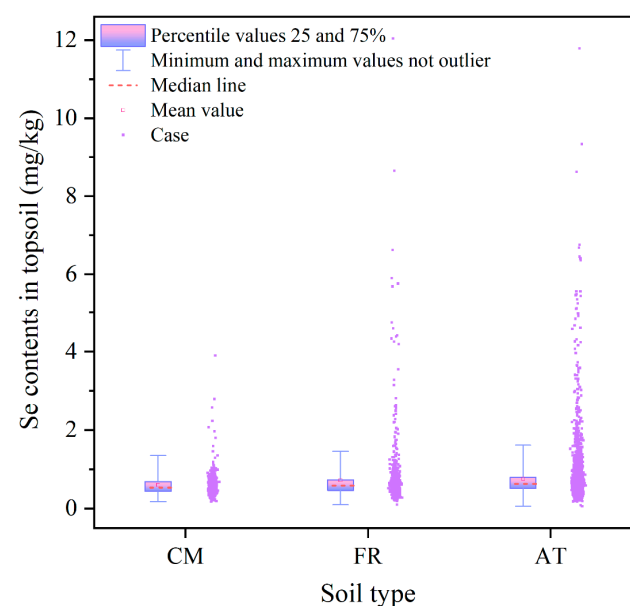


Figure 7. Boxplot of Se contents in topsoil according to soil type. Note: CM: Cambisols; FR: Ferralsols; AT: Anthrosols.

3.3.3. Relationship of Soil Properties and Topography with Se Contents in Topsoil

The data for Se content, soil properties (OM and pH), and topographic parameters (H, SL, TWI) do not show normal distributions. Therefore, the Spearman correlation method was chosen in this study to analyze the correlation between Se, soil properties, and topography. The Spearman correlation coefficients between the above parameters are shown in Table 6.

Table 6. Spearman correlation coefficients of Se, soil properties, and topographical parameters in the cultivated land of Lianyuan City.

	Se	OM	pH	H	SL	TWI
Se	1					
OM	0.478 **	1				
pH	0.082 **	0.338 **	1			
H	−0.154 **	−0.107 **	−0.062 **	1		
SL	−0.108 **	−0.052 **	−0.003	0.546 **	1	
TWI	0.053 **	0.063 **	0.012	−0.321 **	−0.559 **	1

Note: OM: organic matter; H: elevation; SL: slope; TWI: topographic wetness index; **: $p < 0.01$.

OM is a crucial component of soil that significantly influences Se content. Se and OM both carry negative charges, potentially leading to mutual repulsion and limiting the adsorption of Se by OM. However, Se can form stable complexes with functional groups in soil OM, including carboxyl and phenol groups. This complexation transcends simple electrostatic adsorption, enabling Se to bind with OM through stronger chemical bonds such as covalent and coordinate bonds, thereby promoting the stable retention of selenium in the soil. Moreover, soil OM provides a growth substrate for microbes, which can reduce selenate (Se^{6+}) to selenite (Se^{4+}) or elemental Se (0), thus decreasing the mobility of Se in the environment [71]. Numerous studies have discovered a positive correlation between soil Se and soil OM [72–74]. Nevertheless, the correlation between soil Se and soil OM was not evident in partial studies influenced by soil type and OM content [75]. The results showed that the Se content in topsoil is significantly positively correlated with OM ($r = 0.478$, $p < 0.01$) (Table 6). According to the second nationwide general soil survey in China [39], topsoil OM in the cultivated land of Lianyuan City was categorized into four grades: very deficient ($\text{OM} < 6 \text{ g/kg}$), deficient ($6 \text{ g/kg} \leq \text{OM} < 10 \text{ g/kg}$), marginal ($10 \text{ g/kg} \leq \text{OM} < 20 \text{ g/kg}$), and moderate ($20 \text{ g/kg} \leq \text{OM} < 30 \text{ g/kg}$). The OM content ranged from 0.11 g/kg to 21.01 g/kg (mean content of 3.79 g/kg), which indicates that the topsoil OM in the cultivated land of Lianyuan City belongs to very deficient. The mean Se content showed an increasing trend when the OM content was below 20 mg/kg (Figure 8b). When the OM content was above 20 mg/kg, the mean Se content suddenly reduced (Figure 8b). Only two soil sampling points with OM content ranging from 20 g/kg to 30 g/kg were found (Figure 8a). Therefore, the mean Se content is not representative ($2 < \text{total sample of } 5516$) of soil with a moderate OM level ($20 \text{ g/kg} \leq \text{OM} < 30 \text{ g/kg}$). On the whole, the higher the OM content in soil, the more enriched the soil is with Se.

In acidic conditions, selenite (Se^{4+}) is the principal inorganic phase, exhibiting greater stability than selenate (Se^{6+}). Additionally, selenite (Se^{4+}) is readily adsorbed by soil components such as clay minerals, iron oxides, and OM, making selenite (Se^{4+}) resistant to leaching [1]. Therefore, Se content in soil generally increases with decreases in pH. There was a significant positive correlation between pH and Se in this study (Table 6), but the correlation coefficient between pH and Se was very small ($r = 0.082$, $p < 0.01$), indicating the negligible impact of pH on Se content (Figure 8c). Based on the specifications of geochemical assessments of land quality across China [38], the topsoil pH of cultivated land in Lianyuan City was divided into the following categories: strong acidity ($\text{pH} < 5.0$), acidity ($5.0 \leq \text{pH} < 6.5$), neutral ($6.5 \leq \text{pH} < 7.5$), alkalinity ($7.5 \leq \text{pH} < 8.5$), and strong alkalinity ($\text{pH} \geq 8.5$). The average Se content showed no significant change when the pH was less than 8.5 (Figure 8d), whereas when the $\text{pH} \geq 8.5$, the average Se content suddenly

increased. (Figure 8d). Likewise, soil samples with $\text{pH} \geq 8.5$ were few (<10) (Figure 8c), so the data are not representative. In Lianyuan City, the climate is humid, and rainfall is plentiful. High precipitation leads to the leaching of Se, even when Se is in a stable form. As a result, changes in Se forms due to pH have negligible effects on the total Se content. It was tentatively inferred that the extremely weak positive correlation between pH and Se resulted from high precipitation. In order to investigate the exact driving factor of this result, further investigation should explore the correlation between pH and different forms of Se [19].

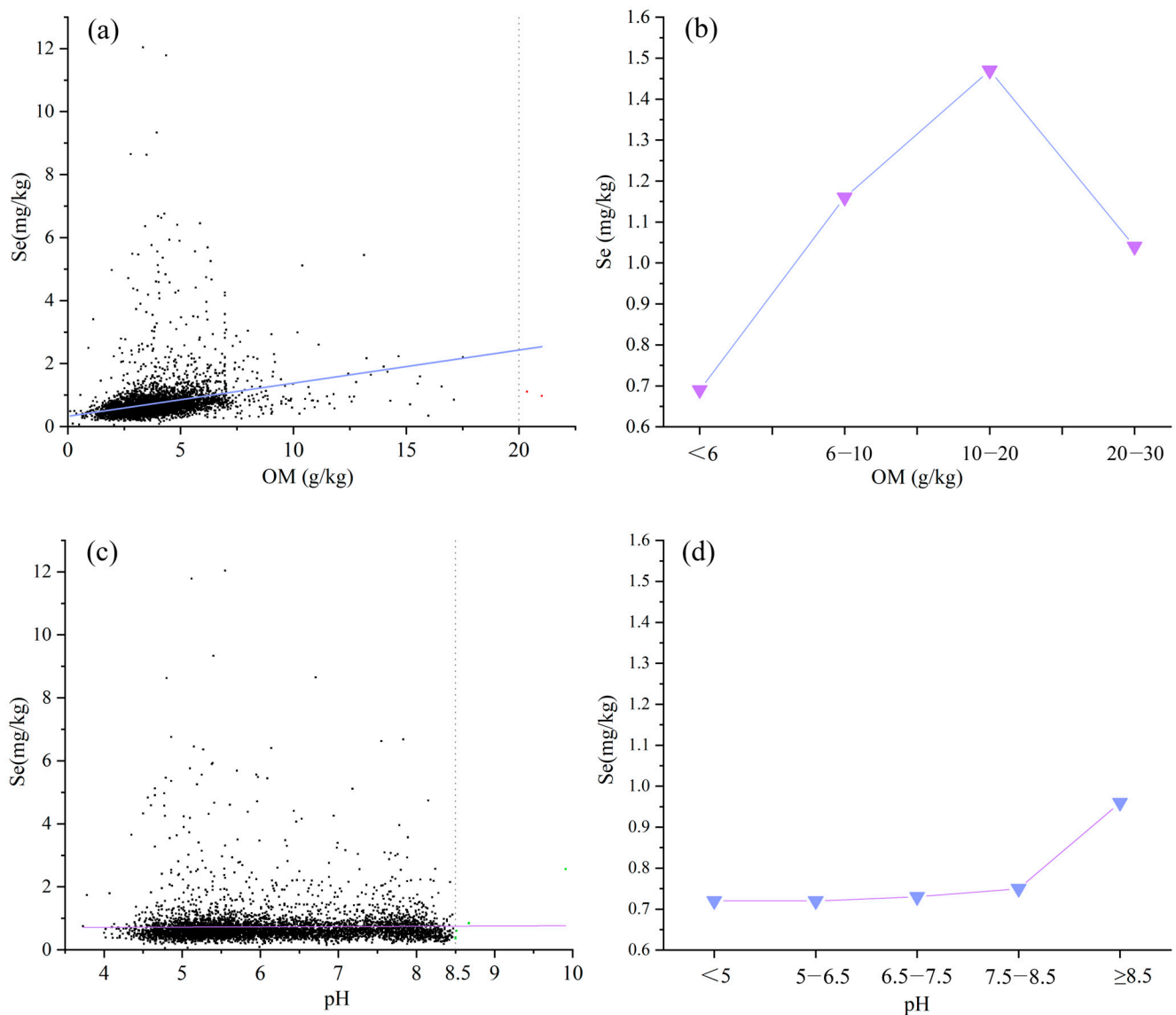


Figure 8. (a) Relationships between Se content and OM in topsoil; (b) the mean Se content in topsoil samples at different OM levels; (c) relationships between Se content and pH in topsoil; (d) the mean Se content in topsoil samples at different pH levels. Note: red points represent sampling points of $20 \text{ g/kg} \leq \text{OM} < 30 \text{ g/kg}$; green points represent sampling points of $\text{pH} > 8.5$.

Topography is considered as one of the major factors affecting soil formation, which indirectly influences the properties and material composition of soil. In our study, H, SL, and TWI were selected as the basic parameters used to quantify the effect of topography on soil Se content. H and SL are the basic topographic parameters that influence surface physical transmission and are used to reflect topographic relief. Shang et al. found that Se was carried to the low-lying areas through the scouring action of surface runoff, causing

soil Se content to decrease with an increase in elevation [76]. Additionally, soil erosion is more likely to occur when the SL is steeper, resulting in Se migration in the form of soil particles [77]. Both H ($r = -0.154, p < 0.01$) and SL ($r = 0.108, p < 0.01$) exhibited a significant positive correlation with Se in soil, in line with Zhu et al. [78]. Similarly, both H ($r = -0.107, p < 0.01$) and SL ($r = -0.052, p < 0.01$) were negatively correlated with the OM in soil. This suggests that the migration of OM and Se in soil is controlled by topography. Compared with high and steep mountainous areas, Se is more commonly enriched in flat and low-lying areas, consistent with John et al. [79].

TWI is an index used to quantify soil moisture conditions, and it is often used to express the influence of topography on soil moisture in a certain place. The larger the value of TWI, the higher the soil water content. There is a significant but weakly positive correlation between Se and TWI. When TWI is high, the soil is in a reduced state, causing Se to primarily exist as sparingly soluble compounds (such as selenide), which limits the efficiency of Se absorption by plant roots, potentially leading to an increase in total soil Se content [80]. Conversely, when TWI is low, soil is in an oxidized state. Se is primarily present in the form of selenate (Se^{6+}) and selenite (Se^{4+}), which are more soluble and readily absorbed by plant roots than selenide, thus resulting in decreased Se content in the soil [81].

3.4. Driving Factors of Spatial Distribution for Topsoil Se

The Geodetector method is based on discretized data to identify the explanatory variable that makes a remarkable contribution to the dependent variable. Factor detection and interaction detection were performed with Geodetector. Factor detection was utilized to detect how much of the spatial variation in attribute Y can be explained by a given factor. The strength of each impact factor on Se was different. The analysis showed that stratum had the highest degree of influence on soil Se content ($q = 0.109$), followed by OM ($q = 0.088$), H ($q = 0.026$), SL ($q = 0.008$), and ST ($q = 0.007$) (Table 7). These results imply that the stratum has a key impact on Se enrichment or Se deficiency in the soil. The Permian in Lianyuan City developed an Se-rich black rock series that provide abundant Se resources for Se-rich soil. A number of studies have concluded that the parent material is the most critical factor influencing soil Se content [10,14]. The results of factor detection again prove the above conclusion. The P value of pH and TWI was greater than 0.01, suggesting that pH and TWI had no significant effect on the spatial differences in soil Se content, in line with the results of the correlation analysis (Table 6).

Table 7. Factor detection of soil Se relative to affecting factor.

	S	ST	OM	pH	H	SL	TWI
q	0.109 ***	0.007 ***	0.088 ***	0.004	0.026 ***	0.008 ***	0.002
p	0.000	0.000	0.000	0.054	0.000	0.000	0.236

Note: S: stratum; ST: soil type; OM: organic matter; H: elevation; SL: slope; TWI: topographic wetness index; ***, $p < 0.01$.

Interactive detection is used to determine whether there is an interaction between impact factors. The results of interactive detection are shown in Figure 9. The interaction strength of two factors is greater than that of one factor, showing bivariate enhancement or nonlinear enhancement (no independent effect). It means that the combined action of two factors increases the impact on Se. The interaction value (q) between the stratum and other factors was relatively high, ranging from 0.118 to 0.196. The stratum and OM had the highest interaction value (q) of 0.196. These data indicate that the soil Se is affected by a combination of stratum, OM, soil type, and topography. In addition, it is worth noting that the synergistic effect of stratum and OM is the dominant factor influencing Se enrichment in the topsoil of cultivated land in Lianyuan City.

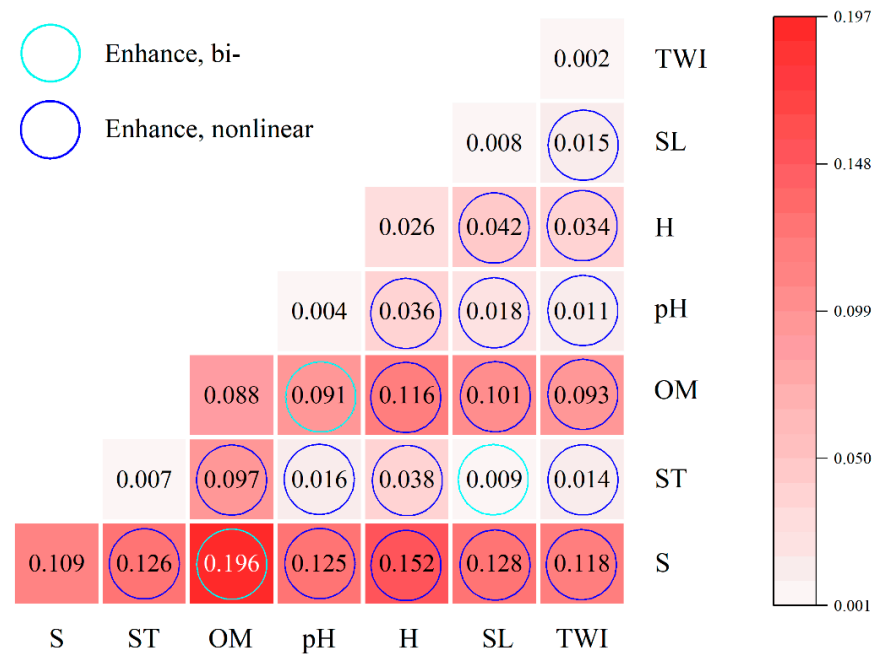


Figure 9. Effect on soil Se after interactions between affecting factors. Note: S: stratum; ST: soil type; OM: organic matter; H: elevation; SL: slope; TWI: topographic wetness index.

4. Conclusions

In this paper, geostatistics were applied to analyze the content and spatial distribution of Se in the topsoil of cultivated land in Lianyuan City. The results demonstrate that the soil Se content in the study area is high, with Se-sufficient and Se-rich areas accounting for 9.74% and 88.96% of the total, respectively. The high level of Se in soil reduces the risk of local residents suffering with diseases caused by Se deficiency. However, crops grown in areas with excessive Se should be tested in order to prevent possible poisoning resulting from the consumption of products with undesirable amounts of Se. The key factors influencing Se content were identified through correlation analysis and using the Geodetector. Our analysis shows that the synergistic effect of stratum and OM has the predominant influence on Se enrichment in soil. The black rock series developed from the Longtan Formation and Dalong Formation contributes Se to the soil, while the presence of OM facilitates the preservation of Se. Furthermore, low-lying flat areas are more conducive to the accumulation of Se. These findings provide an important scientific basis for the development of Se-rich agriculture and the enhancement of human health.

Author Contributions: Literature search, S.G. and X.C.; data collection, processing and analysis, Z.L., K.L. and P.J.; article design, article conception and first draft writing, S.G., X.C. and Z.L.; translating and correcting grammar, X.C. and F.Y.; article format modification and picture processing, K.L. and P.J.; project administration, S.G. and F.Y. All authors have read and agreed to the published version of the manuscript.

Funding: This research was funded by the Postgraduate Scientific Research Innovation Project of Hunan Province (grant number QL20220232) and the Leading Talent Program of Geological Bureau of Hunan Province (grant number HNGSTP202320).

Institutional Review Board Statement: Not applicable.

Data Availability Statement: The data of the multi-purpose regional geochemical survey conducted in the Lou Shao basin of Hunan Province are not publicly available due to confidentiality. Publicly available datasets were analyzed in this study. Geological data can be found here: [<http://www.ngac.org.cn/>] accessed on 20 October 2023, soil type data can be found here: [<http://vdb3.soil.csdb.cn/>] accessed on 20 October 2023, and Digital Elevation Mode (DEM) data can be found here: [<https://www.gscloud.cn/>] accessed on 20 October 2023.

Acknowledgments: We acknowledge all the reviewers who have participated in the review process.

Conflicts of Interest: The authors declare no conflicts of interest.

References

1. Matos, R.P.; Lima, V.M.P.; Windmüller, C.C.; Nascentes, C.C. Correlation between the natural levels of selenium and soil physicochemical characteristics from the Jequitinhonha Valley (MG), Brazil. *J. Geochem. Explor.* **2017**, *172*, 195–202. [[CrossRef](#)]
2. Mao, J.; Pop, V.J.; Bath, S.C.; Vader, H.L.; Rayman, M.P. Effect of low-dose selenium on thyroid autoimmunity and thyroid function in UK pregnant women with mild-to-moderate iodine deficiency. *Eur. J. Nutr.* **2014**, *55*, 55–61. [[CrossRef](#)] [[PubMed](#)]
3. Chang, C.; Zhang, H.; Huang, F.; Feng, X. Understanding the translocation and bioaccumulation of cadmium in the Enshi seleniferous area, China: Possible impact by the interaction of Se and Cd. *Environ. Pollut.* **2022**, *300*, 118927. [[CrossRef](#)] [[PubMed](#)]
4. Huang, Y.; Wang, Q.; Gao, J.; Lin, Z.; Bañuelos, G.; Yuan, L.; Yin, X. Daily dietary selenium intake in a high selenium area of Enshi, China. *Nutrients* **2013**, *5*, 700–710. [[CrossRef](#)] [[PubMed](#)]
5. Roman, M.; Jitaru, P.; Barbante, C. Selenium biochemistry and its role for human health. *Metallomics* **2014**, *6*, 25–54. [[CrossRef](#)] [[PubMed](#)]
6. Rayman, M.P.; Winther, K.H.; Pastor-Barriuso, R.; Cold, F.; Thvilum, M.; Stranges, S.; Guallar, E.; Cold, S.R. Effect of long-term selenium supplementation on mortality: Results from a multiple-dose, randomised controlled trial. *Free Radic. Biol. Med.* **2018**, *127*, S0891584918300704. [[CrossRef](#)] [[PubMed](#)]
7. Kristal, A.R.; Darke, A.K.; Morris, J.S.; Tangen, C.M.; Goodman, P.J.; Thompson, I.M.; Meyskens Jr, F.L.; Goodman, G.E.; Minasian, L.M.; Parnes, H.L.; et al. Baseline selenium status and effects of selenium and vitamin e supplementation on prostate cancer risk. *J. Natl. Cancer Inst.* **2014**, *106*, djt456. [[CrossRef](#)] [[PubMed](#)]
8. Liu, W.; Wu, Y.; Zhong, Y.; Zhao, H. Concentrations, distribution and influencing factors of selenium (Se) in soil of arid and semi-arid climate: A case from Zhangye-Yongchang region, north-western China. *J. Geochem. Explor.* **2023**, *250*, 107239. [[CrossRef](#)]
9. Shahid, M.; Niazi, N.K.; Khalid, S.; Murtaza, B.; Bibi, I.; Rashid, M.I. A critical review of selenium biogeochemical behavior in soil-plant system with an inference to human health. *Environ. Pollut.* **2018**, *234*, 915–934. [[CrossRef](#)]
10. Pan, Z.; He, S.; Li, C.; Men, W.; Yan, C.; Wang, F. Geochemical characteristics of soil selenium and evaluation of Serich land resources in the central area of Guiyang City, China. *Acta Geochim.* **2017**, *2*, 240–249. [[CrossRef](#)]
11. Liu, H.; Wang, X.; Zhang, B.; Han, Z.; Wang, W.; Chi, Q.; Zhou, J.; Nie, L.; Xu, S.; Liu, D.; et al. Concentration and distribution of selenium in soils of mainland China, and implications for human health. *J. Geochem. Explor.* **2021**, *220*, 106654. [[CrossRef](#)]
12. Dinh, Q.T.; Cui, Z.; Huang, J.; Tran, T.A.T.; Wang, D.; Yang, W.; Zhou, F.; Wang, M.; Yu, D.; Liang, D. Selenium distribution in the Chinese environment and its relationship with human health: A review. *Environ. Int.* **2018**, *112*, 294–309. [[CrossRef](#)]
13. Wang, J.; Li, H.; Yang, L.; Li, Y.; Wei, B.; Yu, J.; Feng, F. Distribution and translocation of selenium from soil to highland barley in the Tibetan Plateau Kashin-Beck disease area. *Environ. Geochem. Health* **2017**, *39*, 221–229. [[CrossRef](#)]
14. Jia, M.; Zhang, Y.; Huang, B.; Zhang, H. Source apportionment of selenium and influence factors on its bioavailability in intensively managed greenhouse soil: A case study in the east bank of the Dianchi Lake, China. *Ecotoxicol. Environ. Saf.* **2018**, *170*, 238–245. [[CrossRef](#)]
15. Zhang, M.; Sun, Y. Source of selenium in Handan geochemical anomaly belt: Evidences from petrology and geochemistry of Upper Paleozoic in western Handan, China. *J. Geochem. Explor.* **2021**, *226*, 106770. [[CrossRef](#)]
16. Li, M.; Yang, B.; Xu, K.; Zheng, D.; Tian, J. Distribution of Se in the rocks, soil, water and crops in Enshi County, China. *Appl. Geochem.* **2020**, *122*, 104707. [[CrossRef](#)]
17. Ni, R.; Luo, K.; Tian, X.; Yan, S.; Zhong, J.; Liu, M. Distribution and geological sources of selenium in environmental materials in Taoyuan County, Hunan Province, China. *Environ. Geochem. Health* **2016**, *38*, 927–938. [[CrossRef](#)]
18. Xia, F.; Zhang, X.; Yang, Y.; Chen, P.; Liu, B. Geochemical characteristics and influencing factors of selenium in soils and agricultural products in Ningguo City, Anhui Province. *Trans. Chin. Soc. Agric. Eng. Trans. CSAE* **2021**, *53*, 585–593. [[CrossRef](#)]
19. do Nascimento, C.W.A.; da Silva, F.B.V.; Neta, A.D.B.F.; Biondi, C.M.; da Silva Lins, S.A.; de Almeida Júnior, A.B.; Preston, W. Geopedology-climate interactions govern the spatial distribution of selenium in soils: A case study in northeastern Brazil. *Geoderma* **2021**, *399*, 115119. [[CrossRef](#)]
20. Xiao, K.; Lu, L.; Tang, J.; Chen, H.; Li, D.; Liu, Y. Parent material modulates land use effects on soil selenium bioavailability in a selenium-enriched region of southwest China. *Geoderma* **2020**, *376*, 114554. [[CrossRef](#)]
21. Yu, T.; Hou, W.; Hou, Q.; Ma, W.; Xia, X.; Li, Y.; Yan, B.; Yang, Z. Safe utilization and zoning on natural selenium-rich land resources: A case study of the typical area in Enshi County, China. *Environ. Geochem. Health* **2020**, *42*, 2803–2818. [[CrossRef](#)]
22. Tabelin, C.B.; Igarashi, T.; Villacorte-Tabelin, M.; Park, I.; Opiso, E.M.; Ito, M.; Hiroyoshi, N. Arsenic, selenium, boron, lead, cadmium, copper, and zinc in naturally contaminated rocks: A review of their sources, modes of enrichment, mechanisms of release, and mitigation strategies. *Sci. Total Environ.* **2018**, *645*, 1522–1553. [[CrossRef](#)]
23. Xie, T.; Shi, Z.; Gao, Y.; Tan, L.; Meng, L. Modeling analysis of the characteristics of selenium-rich soil in heavy metal high background area and its impact on main crops. *Ecol. Inform.* **2021**, *66*, 101420. [[CrossRef](#)]
24. Wang, Z.; Gao, Y. Biogeochemical cycling of selenium in Chinese environments. *Appl. Geochem.* **2001**, *16*, 1345–1351. [[CrossRef](#)]

25. Liu, Y.; Liu, S.; Zhao, W.; Xia, C.; Wu, M.; Wang, Q.; Wang, Z.; Jiang, Y.; Zuza, A.V.; Tian, X. Assessment of heavy metals should be performed before the development of the selenium-rich soil: A case study in China. *Environ. Res.* **2022**, *210*, 112990. [[CrossRef](#)]
26. Xu, Y.; Hao, Z.; Li, Y.; Li, H.; Wang, L.; Zang, Z.; Liao, X.; Zhang, R. Distribution of selenium and zinc in soil-crop system and their relationship with environmental factors. *Chemosphere* **2020**, *242*, 125289. [[CrossRef](#)]
27. Odom, F.; Gikunoo, E.; Arthur, E.K.; Agyemang, F.O.; Mensah, D.K. Stabilization of heavy metals in soil and leachate at Dompouse landfill site in Ghana. *Environ. Chall.* **2021**, *5*, 100308. [[CrossRef](#)]
28. Fan, R.; Ni, Z.; Lin, Q.; Huang, Z.; Li, G. Geochemical characteristics and influencing factors of selenium in surface soil of Yongfu County, Guangxi. *Trans. Chin. Soc. Agric. Eng. Trans. CSAE* **2021**, *37*, 15–19. [[CrossRef](#)]
29. Gong, J.; Yang, J.; Wu, H.; Fu, Y.; Gao, J.; Tang, S.; Ma, S. Distribution of soil selenium and its relationship with parent rocks in Chengmai County, Hainan Island, China. *Appl. Geochem.* **2022**, *136*, 105147. [[CrossRef](#)]
30. Xiao, K.; Tang, J.; Chen, H.; Li, D.; Liu, Y. Impact of land use/land cover change on the topsoil selenium concentration and its potential bioavailability in a karst area of southwest China. *Sci. Total Environ.* **2020**, *708*, 135201. [[CrossRef](#)]
31. Xu, Y.; Li, Y.; Li, H.; Wang, L.; Liao, X.; Wang, J.; Kong, C. Effects of topography and soil properties on soil selenium distribution and bioavailability (phosphate extraction): A case study in Yongjia County, China. *Sci. Total Environ.* **2018**, *633*, 240–248. [[CrossRef](#)]
32. Wan, H.; Zhang, W.; Wu, W.; Liu, H. The controlling factors of soil selenium content in a selenium-deficient area in Southwest China. *Agronomy* **2023**, *13*, 1031. [[CrossRef](#)]
33. GB/T 15772-2008; Comprehensive Control of Soil and Water Conversation—General Rule of Planning. General Administration of Quality Supervision, Inspection and Quarantine of the People’s Republic of China: Beijing, China, 2008.
34. Beven, K.J.; Kirby, M. A physically based variable contributing area model of basin hydrology. *Hydrol. Sci. J.* **1979**, *24*, 43–69. [[CrossRef](#)]
35. Wang, J.; Xu, C. Geodetector: Principle and prospective. *Acta Geogr. Sin.* **2017**, *72*, 116–134. [[CrossRef](#)]
36. Chen, X. *Regional Geology of Hunan Province*; The Bureau of Geology and Mineral Resources of Hunan Province, Geology Publishing House: Changsha, China, 1988.
37. Deckers, J.A.; Driessen, P.M.; Nachtergaele, F.O.; Spaargaren, O.C. World Reference Base for Soil Resources. In *Soils of Tropical Forest Ecosystems Characters Ecology & Management*; CRC Press: Boca Raton, FL, USA, 2016; Volume 41, pp. 21–28.
38. DZ/T 0295-2016; Specification of Land Quality Geochemical Assessment. Ministry of Land and Resources of the People’s Republic of China: Beijing, China, 2016.
39. Xing, Q.; Rao, L.; Wang, Z.; Hu, J.; Xu, Y. Characteristics of soil organic matter and available potassium in different types of pisha sandstone area of Inner Mongolia. *J. Soil Water Conserv.* **2019**, *33*, 257–264. [[CrossRef](#)]
40. Wilding, L.P. *Spatial Variability: Its Documentation, Accommodation and Implication to Soil Surveys*; Spatial Variations; PUDOC: Wageningen, The Netherlands, 1985.
41. Yamada, H.; Kamada, A.; Usuki, M.; Yanai, J. Total selenium content of agricultural soils in Japan. *Soil Sci. Plant Nutr.* **2009**, *55*, 616–622. [[CrossRef](#)]
42. Shand, C.A.; Balsam, M.; Hillier, S.J.; Hudson, G.; Newman, G.; Arthur, J.R.; Nicol, F. Aqua regia extractable selenium concentrations of some Scottish topsoils measured by ICP-MS and the relationship with mineral and organic soil components. *J. Sci. Food Agric.* **2010**, *90*, 972–980. [[CrossRef](#)]
43. Ludwig, D.T.; Nadia, W.; Céline, T.; Gijs, D.L.; Filip, T.; Ruttens, A. Selenium content of Belgian cultivated soils and its uptake by field crops and vegetables. *Sci. Total Environ.* **2014**, *468–469*, 77–82. [[CrossRef](#)]
44. Shand, C.A.; Eriksson, J.; Dahlin, A.S.; Lumsdon, D.G. Selenium concentrations in national inventory soils from Scotland and Sweden and their relationship with geochemical factors. *J. Geochem. Explor.* **2012**, *121*, 4–14. [[CrossRef](#)]
45. Wang, Q.; Liu, Q.; Liu, H.; Hu, H.; Wu, H.; Wang, Y. The key elements and life health: Is the cultivated land in China selenium-deficient? *Trans. Chin. Soc. Agric. Eng. Trans. CSAE* **2021**, *28*, 12. [[CrossRef](#)]
46. Xiao, K.; Xu, H.; Li, Y.; Guo, W.; Dai, L.; Peng, Z.; Gong, H.; Xu, Q. Characteristics and influencing factors of soil se content in cultivated land in Longshan County, Hunan Province. *Trans. Chin. Soc. Agric. Eng. Trans. CSAE* **2024**, *42*, 464–474. [[CrossRef](#)]
47. Liu, R.; Zhou, W.; Peng, S.; Shang, G.; Zhou, Y.; Li, M. Characteristics and Influencing Factors of Soil Selenium in Shimen County, Hunan Province. *Trans. Chin. Soc. Agric. Eng. Trans. CSAE* **2023**, *54*, 840–847. [[CrossRef](#)]
48. Wang, J.; Li, H.; Yang, L.; Gong, H.; Li, Y.; Zhao, S.; Ni Ma, C. Selenium in environment and its relationship with Kashin-Beck disease in Chamdo Area of Tibet. *Trans. Chin. Soc. Agric. Eng. Trans. CSAE* **2017**, *36*, 8. [[CrossRef](#)]
49. Zhang, B.; Yang, L.; Wang, W.; LI, Y.; LI, H. Selenium in environment and its relationship with Kaschin-Beck Disease in Rangtang County, Sichuan Province. *Trans. Chin. Soc. Agric. Eng. Trans. CSAE* **2009**, *28*, 6. [[CrossRef](#)]
50. Du, Y.; Luo, K.; Ni, R.; Hussain, R. Selenium and hazardous elements distribution in plant-soil-water system and human health risk assessment of Lower Cambrian, Southern Shaanxi, China. *Environ. Geochem. Health* **2018**, *40*, 2049–2069. [[CrossRef](#)]
51. Zhu, J.; Wang, N.; Li, S.; Li, L.; Su, H.; Liu, C. Distribution and transport of selenium in Yutangba, China: Impact of human activities. *Sci. Total Environ.* **2008**, *392*, 252–261. [[CrossRef](#)]
52. Liu, Y.; Tian, X.; Liu, R.; Liu, S.; Zuza, A.V. Key driving factors of selenium-enriched soil in the low-Se geological belt: A case study in Red Beds of Sichuan Basin, China. *Catena* **2021**, *196*, 104926. [[CrossRef](#)]

53. Shao, Y.; Cai, C.; Zhang, H.; Fu, W.; Zhong, X.; Tang, S. Controlling factors of soil selenium distribution in a watershed in Se-enriched and longevity region of South China. *Environ. Sci. Pollut. Res.* **2018**, *25*, 20048–20056. [[CrossRef](#)]
54. Gong, J.; Yang, J.; Wu, H.; Gao, J.; Tang, S.; Ma, S. Spatial distribution and environmental impact factors of soil selenium in Hainan Island, China. *Sci. Total Environ.* **2022**, *811*, 151329. [[CrossRef](#)]
55. Fairweather-Tait, S.J.; Bao, Y.; Broadley, M.R.; Collings, R.; Ford, D.; Hesketh, J.E.; Hurst, R. Selenium in human health and disease. *Antioxid. Redox Signal.* **2011**, *14*, 1337–1383. [[CrossRef](#)]
56. Jiang, C.; Zhou, W.; Yang, L.; Yan, J.; Tu, S.; Yuan, Y.; Wang, D.; Cheng, H. Geochemical relationship and profile distribution of Selenium and Cadmium in typical Selenium-enriched areas in Enshi. *Chemosphere* **2023**, *338*, 139423. [[CrossRef](#)]
57. Shao, L.Y.; Yang, Z.Y.; Shang, X.X.; Xiao, Z.H.; Wang, S.; Zhang, W.L.; Zheng, M.Q.; Lu, J. Lithofacies palaeogeography of the Carboniferous and Permian in the Qinshui Basin, Shanxi Province, China. *J. Palaeogeogr.* **2015**, *4*, 384–412. [[CrossRef](#)]
58. Hou, H.; Shao, L.; Wang, S.; Xiao, Z.; Wang, X.; Zhen, L.I.; Guangyuan, M.U. Influence of depositional environment on coalbed methane accumulation in the Carboniferous-Permian coal of the Qinshui Basin, northern China. *Front. Earth Sci.* **2019**, *13*, 16. [[CrossRef](#)]
59. Ren, H.; Yang, R. Distribution and controlling factors of selenium in weathered soil in Kaiyang County, Southwest China. *Chin. J. Geochem.* **2014**, *33*, 300–309. [[CrossRef](#)]
60. Dong, L.; Huang, Y.; Li, W.; Duan, C.; Luo, M. Understanding hydrothermal activity and organic matter enrichment with the geochemical characteristics of black shales in Lower Cambrian, Northwestern Hunan, South China. *Lithosphere* **2022**, *2022*, 2241381. [[CrossRef](#)]
61. Qin, M.; Cao, Z.; Guo, J.; Huang, Y.; Sun, L.; Dong, L. Characteristics of shale reservoir and sweet spot identification of the Lower Cambrian Niutitang Formation in Northwestern Hunan Province, China. *Acta Geol. Sin. (Engl. Ed.)* **2019**, *93*, 573–587. [[CrossRef](#)]
62. He, W.; Dai, D.; Ren, B.; Tang, Z.; Qiu, Y. Heavy metal regularity of Carboniferous weathered black shale in Qiziqiao Area, Central Hunan. *Minerals* **2023**, *13*, 1044. [[CrossRef](#)]
63. Xiao, Z.; Liu, J.; Tan, J.; Yang, R.; Hilton, J.; Zhou, P.; Wang, Z.; Cao, Y. Geologic characterization of a lower Cambrian marine shale: Implications for shale gas potential in northwestern Hunan, South China. *Interpretation* **2018**, *6*, T635–T647. [[CrossRef](#)]
64. Wang, L.; Ju, Y.; Liu, G.; Chou, C.L.; Zheng, L.; Qi, C. Selenium in Chinese coals: Distribution, occurrence, and health impact. *Environ. Earth Sci.* **2010**, *60*, 1641–1651. [[CrossRef](#)]
65. Cui, Z.; Huang, J.; Peng, Q.; Yu, D.; Wang, S.; Liang, D. Risk assessment for human health in a seleniferous area, Shuang'an, China. *Environ. Sci. Pollut. Res. Int.* **2017**, *24*, 17701–17710. [[CrossRef](#)]
66. Wedepohl, K.H. The composition of the continental crust. *Geochim. Cosmochim. Acta* **1995**, *59*, 1217–1232. [[CrossRef](#)]
67. Xia, W.; Tan, J. A comparative study of selenium content in Chinese rocks. *Trans. Chin. Soc. Agric. Eng. Trans. CSAE* **1990**, *10*, 125–131.
68. Li, B.; Liu, X.; Zhang, C.; Yu, T.; Wu, T.; Zhuo, X.; Li, C.; Wang, L.; Lin, K.; Ma, X.; et al. Spatially varying relationships of soil Se concentration and rice Se concentration in Guangxi, China: A geographically weighted regression approach. *Chemosphere* **2023**, *343*, 140241. [[CrossRef](#)] [[PubMed](#)]
69. Zhou, W.; Yang, Z.; Zhang, T.; Song, X.; Yang, C. Distribution characteristics and influencing factors of Se in selenium-rich cultivated land in Libo, Guizhou. *Trans. Chin. Soc. Agric. Eng. Trans. CSAE* **2022**, *42*, 585–592. [[CrossRef](#)]
70. Jia, S. Evaluation standards and genesis of selenium-rich soil in Anhui Province. *Trans. Chin. Soc. Agric. Eng. Trans. CSAE* **2013**, *34*, 5. [[CrossRef](#)]
71. Li, Z.; Liang, D.; Peng, Q.; Cui, Z.; Huang, J.; Lin, Z. Interaction between selenium and soil organic matter and its impact on soil selenium bioavailability: A review. *Geoderma* **2017**, *295*, 69–79. [[CrossRef](#)]
72. Li, X.; Chang, S.X.; Liu, J.; Zheng, Z.; Wang, X. Soil selenium enrichment in the Loess Plateau of China: Geogenic evidence, spatial distribution, and its influence factors. *Chemosphere* **2023**, *340*, 139846. [[CrossRef](#)] [[PubMed](#)]
73. Lei, W.; Cicchella, D.; Liu, T.; Yang, S.; Zhou, Y.; Hu, B.; Liu, Y.; Lin, X. Origin, distribution and enrichment of selenium in oasis farmland of Aksu, Xinjiang, China. *J. Geochem. Explor.* **2021**, *223*, 106723. [[CrossRef](#)]
74. Li, X.; Chang, S.X.; Liu, J.; Zheng, Z.; Wang, X. Topography-soil relationships in a hilly evergreen broadleaf forest in subtropical China. *J. Soil Sediments* **2017**, *17*, 1101–1115. [[CrossRef](#)]
75. Carvalho, G.S.; Oliveira, J.R.; Curi, N.; Schulze, D.C.; Marques, J.J. Selenium and mercury in Brazilian Cerrado soils and their relationships with physical and chemical soil characteristics. *Chemosphere* **2019**, *218*, 412–415. [[CrossRef](#)]
76. Shang, G.; Zhou, W.; Zheng, C.; Liu, R.; Xu, Z.; Cui, H.; Zhou, Y.; Li, M. Spatial distribution of selenium in cultivated soil and its influencing factors in Hunan Province. *Trans. Chin. Soc. Agric. Eng. Trans. CSAE* **2023**, *42*, 2979–2986. [[CrossRef](#)]
77. Chang, H.; Zhu, J.; Lin, Z.; Meng, L. Topographic constraints on the distribution of selenium in the supergene environment: A case study at Yutangba, China. *Environ. Pollut.* **2023**, *319*, 121026. [[CrossRef](#)] [[PubMed](#)]
78. Zhu, J.; Zheng, B. Distribution of selenium in a mini-landscape of Yutangba, Enshi, Hubei Province, China. *Appl. Geochem.* **2001**, *16*, 1333–1344. [[CrossRef](#)]
79. Tuttle, M.L.W.; Fahy, J.W.; Elliott, J.G.; Grauch, R.I.; Stillings, L.L. Contaminants from Cretaceous black shale: I. Natural weathering processes controlling contaminant cycling in Mancos Shale, southwestern United States, with emphasis on salinity and selenium. *Appl. Geochem.* **2014**, *46*, 57–71. [[CrossRef](#)]

80. Liu, X.; Cheng, H.; Cheng, S.; Xu, F.; Rao, S. Advances in research on influencing factors of selenium enrichment in plants. *Plant Growth Regul.* **2023**, 1–13. [[CrossRef](#)]
81. Jones, G.D.; Droz, B.; Greve, P.; Gottschalk, P.; Poffet, D.; McGrath, S.P.; Seneviratne, S.I.; Smith, P.; Winkel, L.H. Selenium deficiency risk predicted to increase under future climate change. *Proc. Natl. Acad. Sci. USA* **2017**, *114*, 2848–2853. [[CrossRef](#)]

Disclaimer/Publisher’s Note: The statements, opinions and data contained in all publications are solely those of the individual author(s) and contributor(s) and not of MDPI and/or the editor(s). MDPI and/or the editor(s) disclaim responsibility for any injury to people or property resulting from any ideas, methods, instructions or products referred to in the content.